VI International Conference on Particle-based Methods – Fundamentals and Applications
PARTICLES 2019
E. Oñate, M. Bischoff, D.R.J. Owen P. Wriggers, , & T. Zohdi (Eds)

APPLICATION OF MIXED MESHLESS SOLUTION PROCEDURES FOR DEFORMATION MODELING IN GRADIENT ELASTICITY

BORIS JALUŠIĆ[1], TOMISLAV JARAK[1] AND JURICA SORIĆ[1]

[1]University of Zagreb, Faculty of Mechanical Engineering and Naval Architecture
Ivana Lučića 5, 10002 Zagreb
boris.jalusic@fsb.hr; tomislav.jarak@fsb.hr, jurica.soric@fsb.hr; www.fsb.hr/lnm

Key words: Mixed MLPG methods, fourth-order differential equation, gradient elasticity

Abstract. The present study is related to the utilization of the mixed Meshless Local Petrov-Galerkin (MLPG) methods for solving problems in gradient elasticity, which are governed by fourth-order differential equations. Here, three different numerical MLPG methods are presented, where the continuity requirements for the approximation functions are lowered by applying different mixed procedures to improve the numerical accuracy and efficiency. The first one is based on the direct solution of the problem, where the primary variable (displacement) and its independently chosen higher-order variables are approximated separately. The global discretized system of equations consists of appropriate equilibrium and compatibility equations written for each node and the solution vector contains all unknown independent nodal variables. Such approach demands only the first-order continuity of meshless approximation functions. The second and third procedures are both based on the displacement-based operator-split approach, where the original gradient elasticity problem is solved as two uncoupled problems governed by the second-order differential equations. Herein, in both uncoupled problems only primary variable (displacement) and its first derivative (strain) are approximated independently. In these procedures the original problem is solved by a staggered approach, where the solution of the first uncoupled equation is utilized as an input in the second equation. The main difference in the second and third procedure is that the one is based on the solution of the local weak forms of the governing equations, while the other is based on solution of the strong forms of the same equations. The accuracy of the presented computational methods is compared to analytical solutions and demonstrated on a one-dimensional benchmark problem of axial bar in gradient elasticity.

1 INTRODUCTION

The solution of the fourth-order differential equations using the Finite Element Method (FEM) results is complicated formulations [1]. When solved using primal FEM, where only primary variable (displacement) is approximated, the C1 continuous shape functions are a necessity, which results in complexity even for two-dimensional problems [2]. On the other hand, if mixed FEM procedures [3] are utilized, the well-known Ladyzhenskaya–Babuška–Brezzi (LBB) conditions [4] need to be satisfied to ensure the stability of the method, and a large number of unknown nodal variables appear. Alternatively, meshless methods have attracted attention due to simple manner of construction of high-order continuity approximations [5]. Nevertheless, the calculation of high-order meshless approximation functions and their derivatives is still a major drawback due to its high computational costs. This can be easily seen in early papers where primal C1 formulations of meshless methods are applied for solving thin beams [6] and plates [7]. Furthermore, weak form primal meshless methods suffer from a further computational deficiency due to the inaccurate integration of the weak forms containing the derivatives of meshless functions [8]. This deficiencies are here alleviated to a certain extent by using the mixed MLPG method paradigm [9].

In this contribution, three different mixed MLPG methods for solving problems in gradient elasticity are proposed. For simplicity, here the proposed approaches are presented only for one-dimensional elasticity, but they can readily be extended to higher dimensional problems. In the first method, the displacement and the higher-order independent variables are approximated separately by the same functions. The governing equations are based on the local weak form of the original strain gradient equation and the compatibility conditions between the approximated variables. In the standard Galerkin weak forms, the Heaviside functions are chosen as the test function leading to the mixed Meshless Finite Volume Method (mMFVM) [10]. Therein, the use of the mixed stratagem lowers the continuity on trial functions and enables the use of lower polynomial bases, which improves numerical stability and reduces computational costs. In this formulation, only the values of nodal shape functions need to be calculated in order to assemble the nodal stiffness matrix. The second and third considered formulations are based on the operator-split solution procedure, where the original gradient elasticity fourth-order differential equation is first decomposed in an uncoupled two sets of the second-order differential equations [11], for the purpose of decreasing the continuity requirement on the trial functions. Hence, two different boundary value problems, local (classical) and non-local (gradient), are being solved, where the solution of the former problem is used as an input in the latter one. The continuity requirements for trial functions are further lowered by separately approximating displacements and their first derivatives in each decoupled equation set. In the second procedure which is based on the use of the local weak forms of the governing equations the application of the operator-split solution scheme [12], utilizing the mixed meshless approach, results in a C0 meshless formulation. Hence, within this approach only the values of nodal shape functions need to be computed to assemble coefficient matrices. In comparison, in the third procedure where the strong forms of the governing equations are being used the calculation of the first-order derivatives of shape functions is necessary in order to assemble the coefficient matrices.

The paper is organized as follows: Section 2 is related to the overview of the governing equations for one-dimensional gradient elasticity for three different solution procedures being considered. The brief description of the utilized Interpolating Moving Least Squares (IMLS) approximation [13] and the derivation of the applied mixed meshless methods are presented in Section 3. One numerical example of axial bar subjected to force in gradient elasticity is analyzed in Section 4. In the last section, concluding remarks on the presented solution procedures are given.

2 GOVERNING EQUATIONS

2.1 Mixed Meshless Finite Volume Method (mMFVM)

In order to present the proposed mixed meshless finite volume procedure, here a general governing equation for a homogeneous axial bar in gradient elasticity

$$Eu'' - l^2 Eu'''' + q = 0, \quad \text{in} \;\; \Omega, \tag{1}$$

is considered. In equation (1), the unknown variable is the displacement u, and the primed symbols denote its derivatives, while q denotes the axial continuous load per unit length. In order to solve the problem, boundary conditions (BCs) on the outer global boundary Γ need to be satisfied. These BCs can be written as

$$\begin{aligned} &u = \bar{u} \;\text{ on }\; \Gamma_u, \;\; P = \bar{t} \;\text{ on }\; \Gamma_P, \Gamma = \Gamma_P \cup \Gamma_u, \Gamma_P \cap \Gamma_u = \varnothing, \\ &R = \bar{R} \;\text{ on }\; \Gamma_R, \;\; Du = \overline{u_{,1}} = \bar{\varepsilon} \;\text{ on }\; \Gamma_{Du}, \Gamma = \Gamma_R \cup \Gamma_{Du}, \Gamma_R \cap \Gamma_{Du} = \varnothing, \end{aligned} \tag{2}$$

where $u_{,1} = \varepsilon$ is the first-order displacement gradient, i.e. strain, and P and R are the tractions and double tractions, respectively, while $\Gamma_u, \Gamma_P, \Gamma_{Du}$ and Γ_R denote parts of Γ with the prescribed values for the displacements, strains, tractions and double tractions, respectively. These tractions are defined as

$$P = t = n(\sigma + \mu) = n(\sigma - \tau_{,1}) = n\tilde{\sigma}, \;\; R = nT = nn\tau = \tau. \tag{3}$$

Herein, t and T stand for the "true" tractions and double tractions, while P and R are their generalized "mathematical" counterparts emerging from the variational formulation of the considered problem. Note that in general the above equality between the "true" and generalized loading variables is not valid, see e.g. [3] for a detailed discussion on that subject. n denotes the outward unit normal vector on the global boundary, and $\tilde{\sigma} = \sigma + \mu$ stands for the true stress, with $\mu = -\tau_{,1}$ is the second-order stress, and τ denotes the double stress. Here it is important to note that the value of R is completely defined by the value of τ, e.g. $\Gamma_R = \Gamma_\tau$.

In this contribution, a simple constitutive law with only one microstructural parameter l is employed. Hence, $\sigma = E\varepsilon = Eu_{,1}$ is the Cauchy stress, and $\tau = l^2 \nabla\sigma = l^2 E u_{,11}$ is the double stress, with E as the Young's modulus. According to the mixed MLPG strategy, the primal displacement u and the variables depending on the displacement gradients may all be regarded as independent variables and approximated separately [9]. In this contribution, the set of variables is chosen so that it simplifies the integrals of the weak form as much as possible, while preserving a clear physical overview. These set of chosen independent variables are as follows

$$u_1 = u, \;\; u_2 = \varepsilon = u', \;\; u_3 = \eta = u'', \;\; u_4 = \mu = -l^2 Eu'''. \tag{4}$$

For simplification the substitutions $\{u, \varepsilon, \eta, \mu\} = \{u_1, u_2, u_3, u_4\}$ are employed in the further text. By using the set of independent variables (4), the original governing equation (1) may be recast into the following system of equations

$$\begin{aligned} &u' - \varepsilon = 0, && \Rightarrow && u_1' - u_2 = 0, \\ &\varepsilon' - \eta = 0, && \Rightarrow && u_2' - u_3 = 0, \\ &\tau_{,1} + \mu = 0, && \Rightarrow && l^2 Eu_3' + u_4 = 0, \\ &(\sigma + \mu)_{,1} + q = 0, && \Rightarrow && Eu_2' + u_4' + q = 0, \end{aligned} \tag{5}$$

where the fourth equation is the equilibrium equation written in terms of stresses, and the first three equations represent the compatibility equations between various independent variables. The local weak forms of the governing equations (5) may now be written for each node as

$$\int_{\Omega_S} v_1\left(u_1'-u_2\right)\mathrm{d}x=0, \qquad \int_{\Omega_S} v_2\left(u_2'-u_3\right)\mathrm{d}x=0,$$
$$\int_{\Omega_S} v_3\left(l^2 E u_3'+u_4\right)\mathrm{d}x=0, \qquad \int_{\Omega_S} v_4\left(E u_2'+u_4'+q\right)\mathrm{d}x=0. \tag{6}$$

In all the above equations the Heaviside functions are chosen as the test functions v_i, $i=1,2,3,4$, leading to the mixed meshless finite volume method (mMFVM).

2.2 Mixed Meshless Finite Volume Operator Split Method (mMFVOSM)

In the second procedure the original fourth-order governing equation (1) is solved as an uncoupled sequence of two differential equations of the second-order. According to [12] the original problem is split into classical (local) governing equation

$$E u_{\mathrm{c}}''+q=0, \quad \text{in } \Omega, \tag{7}$$

and the gradient (non-local) governing equation

$$u_{\mathrm{g}}-l^2 u_{\mathrm{g}}''=u_{\mathrm{c}}, \quad \text{in } \Omega. \tag{8}$$

Herein and in the following, the indices c and g denote the variables and objects referring to the classical (7) or gradient problem (8), respectively. The problem stated by (7) and (8) can be solved in a staggered manner. Firstly the classical problem (7) is solved and thereafter its solutions are used as input in the gradient problem (8). Due to the operator-split procedure the BCs of the original problem (2) have to be modified [11]. The BCs that need to be satisfied when solving (7) and (8) are

$$\begin{aligned} &u_{\mathrm{c}}=\bar{u}_{\mathrm{c}} \text{ on } \Gamma_{\mathrm{c}u}, \quad t_{\mathrm{c}}=\sigma_{\mathrm{c}11} n_{\mathrm{c}}=\bar{t}_{\mathrm{c}} \text{ on } \Gamma_{\mathrm{c}t}, \quad \Gamma_{\mathrm{c}}=\Gamma_{\mathrm{c}u}\cup\Gamma_{\mathrm{c}t},\\ &u_{\mathrm{g}}=\bar{u}_{\mathrm{g}} \text{ on } \Gamma_{\mathrm{g}u}, \quad t_{\mathrm{g}}=l^2 u_{\mathrm{g}}' n_{\mathrm{g}}=\bar{t}_{\mathrm{g}} \text{ on } \Gamma_{\mathrm{g}t}, \quad \Gamma_{\mathrm{g}}=\Gamma_{\mathrm{g}u}\cup\Gamma_{\mathrm{g}t}, \end{aligned} \tag{9}$$

where $\Gamma_{\mathrm{c}u}$ and $\Gamma_{\mathrm{g}u}$ denote parts with the prescribed values of essential BCs of displacements u_{c} and u_{g}, while $\Gamma_{\mathrm{c}t}$ and $\Gamma_{\mathrm{g}t}$ are the parts where natural BCs are applied. These natural BCs include prescribed values of classical traction t_{c} and the second-order traction t_{g}. The local weak forms of the governing equations of the classical (7) and gradient problem (8), after the integration by parts, are written as

$$\begin{aligned} &\int_{\Omega_S} v_{\mathrm{c}}' E u_{\mathrm{c}}' \mathrm{d}x - \int_{\Gamma_S\cup\Gamma_{\mathrm{c}u}} v_{\mathrm{c}} t_{\mathrm{c}} \mathrm{d}x = -\int_{\Omega_S} v_{\mathrm{c}} q \mathrm{d}x + \int_{\Gamma_{\mathrm{c}t}} v_{\mathrm{c}} \bar{t}_{\mathrm{c}} \mathrm{d}x,\\ &\int_{\Omega_S} v_{\mathrm{g}} u_{\mathrm{g}} \mathrm{d}x + \int_{\Omega_S} l^2 v_{\mathrm{g}}' u_{\mathrm{g}}' \mathrm{d}x - \int_{\Gamma_S\cup\Gamma_{\mathrm{g}u}} v_{\mathrm{g}} t_{\mathrm{g}} \mathrm{d}x = \int_{\Omega_S} v_{\mathrm{g}} u_{\mathrm{c}} \mathrm{d}x + \int_{\Gamma_{\mathrm{g}t}} v_{\mathrm{g}} \bar{t}_{\mathrm{g}} \mathrm{d}x. \end{aligned} \tag{10}$$

In the considered operator-split procedure, a mixed meshless paradigm as in [9] is utilized in the classical problem (the first equation in (10)), and the gradient problem is discretized in analogous manner (the second equation in (10)). Accordingly, the classical or gradient displacements and their first-order derivatives (strains), u_c and $\varepsilon_{\mathrm{c}}=u_{\mathrm{c}}'$, or u_g and $\varepsilon_{\mathrm{g}}=u_{\mathrm{g}}'$, respectively, are chosen as the unknown system variables, depending on the equation being solved. All the unknown variables are approximated separately using the same approximation functions. Again, in the weak forms in (10) the Heaviside function may be used as the test function in order to reduce computational costs and to improve the numerical accuracy and stability. It is then obvious that all the natural BCs ($t_c = \bar{t}_c$ on Γ_{ct} and $t_g = \bar{t}_g$ on Γ_{gt}) are enforced in the weak sense. The unknown displacements and the first order derivatives are connected via well-known compatibility equations $\varepsilon_c = u_c'$, $\varepsilon_g = u_g'$. They can be enforced for each node in a weak form over the local subdomain as in mMFVM, see (6), or by means of collocation at the nodes, as in [9]. In the latter case, the size of the global equation system can be reduced relatively easily by eliminating the values of nodal strains from the equations (10), see [8] or [9] for more details. Then, the essential BCs ($u_c = \bar{u}_c$ on Γ_{cu} and $u_g = \bar{u}_g$ on Γ_{gu}) can be satisfied directly as in FEM.

2.3 Mixed Meshless Collocation Operator Split Method (mMCOSM)

The third considered procedure is similar to the second one and is also based on the previously described staggered solution scheme. If the standard Galerkin weak forms of the equations (7) and (8) are written we obtain the local forms of the classical (local)

$$\int_{\Omega_S} v_c \left(E u_c'' + q \right) \mathrm{d}x = 0, \quad \text{in} \ \ \Omega, \tag{11}$$

and gradient (non-local) governing equation

$$\int_{\Omega_S} v_g \left(u_g - l^2 u_g'' - u_c \right) \mathrm{d}x = 0, \quad \text{in} \ \ \Omega. \tag{12}$$

In the above equations the Dirac delta function is chosen as the test function leading to meshless collocation method [14]. In that way, the strong for of the governing equations only at the collocation nodes are obtained

$$E u_c''(x_I) + q(x_I) = 0, \quad \text{in} \ \ \Omega, \tag{13}$$

$$u_g(x_I) - l^2 u_g''(x_I) - u_c(x_I) = 0, \quad \text{in} \ \ \Omega. \tag{14}$$

Solution procedure remains the same as in the second procedure, however there is no need for numerical integration. In the utilized solution procedure the mixed meshless collocation paradigm [15] is used. Herein, the chosen unknown system variables in the solution procedure of the classical problem are u_c and $\varepsilon_c = u_c'$, while in the gradient problem they are u_g and $\varepsilon_g = u_g'$. In order to connect the approximated variables the compatibility equations $\varepsilon_c = u_c'$, $\varepsilon_g = u_g'$ are enforced at the nodes using the collocation method. Furthermore, due to the used staggered solution procedure the BCs of the original problem according to [11] have to be changed. Thus, the BCs that need to be satisfied are

$$u_c = \bar{u}_c, \quad \text{on} \ \Gamma_{cu}, \quad t_c = \sigma_{c11} n_c = \bar{t}_c, \quad \text{on} \ \Gamma_{ct}, \tag{15}$$

$$u_g = \bar{u}_g \quad \text{on} \ \Gamma_{gu}, \quad t_g = n_g^2 u_g'' = \bar{t}_g, \quad \text{on} \ \Gamma_{gt}. \tag{16}$$

The essential BCs are here again enforced directly as in FEM, while the natural BCs are discretized using mixed meshless collocation and satisfied at the collocation nodes as in [16].

3 NUMERICAL IMPLEMENTATION

3.1 Discretization

The global domain Ω in both procedures is discretized by a set of N nodes $x_I, I=1,2,...,N$. Around each node I a local sub-domain Ω_S^I is defined, bounded by a local boundary Γ_S^I, as displayed in Fig.1.

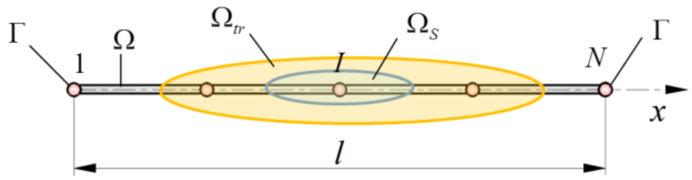

Figure 1: Discretization model

The local weak forms of equations (6) or (10) are written for each Ω_S^I. All the considered unknown variables are approximated using the same meshless approximation scheme. In the first procedure (mMFVM), independently chosen variables u_i from (4) are considered as the unknown variables in (6). Within the mMFVOSM, in the local problem the classical displacement u_c and the classical strain ε_c are approximated, while in the non-local problem gradient displacement u_g and gradient strain ε_g are utilized as unknown variables. Here, the IMLS approximation is used, written as

$$\varphi(x) = \sum_{J=1}^{N} \phi_J(x)(\hat{\varphi})_J . \tag{17}$$

In (17), ϕ_J and $(\hat{\varphi})_J$ represent the one-dimensional (1D) nodal shape function and the nodal value of the approximated variables at node *J*, respectively. According to [17, 18], the nodal shape function $\phi_J(x)$ can be written as

$$\phi_J(x) = \mathbf{p}^\mathrm{T}(x)\left[\mathbf{A}^{-1}(x)\mathbf{B}(x)\right]_J . \tag{18}$$

In equation (18) the momentum matrix $\mathbf{A}(x)$ is

$$\mathbf{A}(x) = \sum_{J=1}^{n} W_J(x)\mathbf{p}(x_J)\mathbf{p}^\mathrm{T}(x_J), \tag{19}$$

while the matrix $\mathbf{B}(x)$ is written as

$$\mathbf{B}(x) = \left[W_1(x)\mathbf{p}(x_1) \quad W_2(x)\mathbf{p}(x_2) \quad \cdots \quad W_J(x)\mathbf{p}(x_J) \quad \cdots \quad W_n(x)\mathbf{p}(x_n)\right]. \tag{20}$$

In order to improve the conditioning of the momentum matrix $\mathbf{A}(x)$, the complete monomial basis $\mathbf{p}$ is written in terms of local normalized coordinates [19]. Within (19) and (20) $W_J(x)$ represents the weight function associated with node *J*. In this contribution the regularized weight function [20] is utilized to ensure the Kronecker delta property, $\phi_J(x_I) \approx \delta_{JI}$. It should be stated that the node I influences the values of the approximated variables only at the points within the weight function support domain Ω_{tr}^{I}.

In the first considered procedure (mMFVM), by inserting approximations defined by (17) into the local weak forms (6), the system consisting of four linear algebraic equations obtained for each node. In the operator split procedure, by using the approximations (17) within the weak forms (10) only one algebraic equation is obtained for a given node in each of the problems considered (local and gradient). For both procedures, a global system of equations is achieved by writing the equations in node-by-node principle [18].

3.2 Discretized equations of the mMFVM

Analogously to the formulation in [10], all the test functions v_i in (6) are chosen to be Heaviside functions. Hence, a form of mixed Meshless Finite Volume Method (mMFVM) is obtained. In order to derive the discretized system of equations for each node, firstly the integration by parts and divergence theorem is applied in all weak forms (6). Secondly, the discretization of the chosen independent variables using IMLS functions [20] is done leading to the final system of equation for the node I

$$\sum_{J=1}^{N}\mathbf{K}_{IJ}\,\hat{\mathbf{U}}_{J}=\mathbf{R}_{I}, \tag{21}$$

where $\mathbf{K}_{IJ}$ is the contribution of the node J to the stiffness of the local subdomain of the node I, Ω_S^I. In (21) $\hat{\mathbf{U}}_J$ denotes the vector consisting of nodal variables at the node J, while $\mathbf{R}_I$ is the nodal force vector at node I. For the chosen independent variables vector $\mathbf{R}_I$ is defined as

$$\mathbf{R}_I=\begin{bmatrix}-\int\limits_{\Gamma_u^I} n\,\overline{u}_1\,\mathrm{d}\Gamma & -\int\limits_{\Gamma_{Du}^I} n\,\overline{u}_2\,\mathrm{d}\Gamma & -\int\limits_{\Gamma_R^I}\overline{T}\,\mathrm{d}\Gamma & -\int\limits_{\Omega_S^I} q\,\mathrm{d}\Gamma-\int\limits_{\Gamma_P^I}\overline{t}\,\mathrm{d}\Gamma\end{bmatrix}^{\mathrm{T}}. \tag{22}$$

In the above equation, n represents the outward unit normal vector to the global boundary, and the prescribed values are defined as

$$\begin{aligned}&\overline{u}_1=\overline{u}, \qquad \overline{u}_2=\overline{\varepsilon}=\overline{u}',\\ &\overline{T}=n\,\overline{\tau}=n\,l^2E\,\overline{u}''=n\,l^2E\,\overline{u}_3,\\ &\overline{t}=n\,\overline{\overline{\sigma}}=n\left(\overline{\sigma}+\overline{\mu}\right)=n\left(E\,\overline{u}'-l^2E\,\overline{u}'''\right)=n\left(E\,\overline{u}_2+\overline{u}_4\right).\end{aligned} \tag{23}$$

Note that the double traction $\overline{R}$ is completely defined by the known value of the double stress $\overline{\tau}$, according to (3). From (22), it is obvious that in this method all BCs are satisfied in a weak form, without the need to introduce special procedures for enforcing BCs, which can be a problem in meshless methods [18]. In addition, all non-zero terms of the matrix $\mathbf{K}_{IJ}$ are integrals over Ω_S^I and the parts of local boundary Γ_S^I, and contain only nodal shape functions. Therefore, the stiffness matrix can be computed without the need of performing costly and inaccurate numerical integration of the derivatives of nodal shape functions.

3.3 Discretized equations of the mMFVOSM

Here again the test functions in both classical v_c and gradient problem v_g are chosen to be Heaviside functions in order to obtain a form of the mMFVOSM. According to the mixed MLPG strategy the local weak forms (10) are firstly discretized by using the approximation (17) for ε_c and ε_g. Next, to obtain the discretized systems of equations with only the classical u_c and gradient u_g displacements as unknowns, the compatibility between the approximated strains and displacements is enforced via the collocation method at the nodes of the model. By employing the compatibility conditions in the discretized form of the local weak forms (10) the nodal strains are eliminated. This nodal elimination can be performed efficiently during the node-by-node assembly of the global system of equations for both the classical and gradient problems. Firstly, the classical problem is assembled and solved, and thereafter, the solution of the classical problem is utilized in the assembly of the gradient system of equations, where the obtained classical displacements appear as the input term in the gradient nodal force vector. The final systems of equations in this procedure can be written as

$$\begin{aligned} &\sum_{J=1}^{N} \mathbf{K}_{IJ}^{c}\,\hat{\mathbf{U}}_{J}^{c} = \mathbf{R}_{I}^{c}, \\ &\sum_{J=1}^{N} \mathbf{K}_{IJ}^{g}\,\hat{\mathbf{U}}_{J}^{g} = \mathbf{R}_{I}^{g}, \end{aligned} \tag{24}$$

where $\mathbf{K}_{IJ}^{c}$ and $\mathbf{K}_{IJ}^{g}$ are the contributions of the node J to the coefficient matrices associated with the local subdomains of node I in the classical and gradient problem, respectively, while the nodal vectors $\hat{\mathbf{U}}_{J}^{c}$ and $\hat{\mathbf{U}}_{J}^{g}$ consist of unknown classical and gradient displacements. Furthermore, the nodal vectors on the right-hand side at node I are equal to

$$\begin{aligned} \mathbf{R}_{I}^{c} &= \left[\int_{\Omega_S^I} q \,\mathrm{d}\Gamma + \int_{\Gamma_{ct}^I} \bar{t}_c \,\mathrm{d}\Gamma \right], \\ \mathbf{R}_{I}^{g} &= \left[\int_{\Omega_S} u_c \mathrm{d}\Gamma + \int_{\Gamma_{gt}} \bar{t}_g \mathrm{d}\Gamma \right]. \end{aligned} \tag{25}$$

As can be seen from (25), the natural BCs are satisfied in the weak sense, similar to the first procedure. Due to the interpolation property of the meshless approximation functions, in both uncoupled problems the essential BCs can be easily imposed, just as in FEM.

3.4 Discretized equations of the mMCOSM

Since the Dirac delta function in chosen as the test function in both classical v_c and gradient problem v_g the form of mMCOSM is achieved. Here, related to the mixed collocation strategy in [16] the strong forms (13) and (14) are firstly discretized utilizing (17) for ε_c and ε_g. Furthermore, in order to obtain the closed solvable systems of equations with only the classical u_c and gradient displacements u_g as unknowns, the compatibility between the approximated strains and displacements in enforced using the collocation method. As in the second procedure, the classical problem is firstly assembled and solved. The solution of the classical problem is then used as input in the subsequent assembly and solution of the gradient problem. The obtained final system of equations in this procedure can also be written analogous to equations given by (24). In addition, at the nodes where the natural boundary conditions are present the system equations are replaced by discretized boundary conditions at the node *I*. The BCs are discretized using mixed collocation and can be written as

$$\mathbf{R}_I^{\mathrm{c}} = nE\sum_{J=1}^{N}\mathbf{B}_{IJ}^{\mathrm{c}}\,\hat{\mathbf{U}}_J^{\mathrm{c}},$$
$$\mathbf{R}_I^{\mathrm{g}} = n^2\sum_{K=1}^{N}\mathbf{H}_{FK}^{\mathrm{g}}\sum_{J=1}^{N}\mathbf{G}_{KJ}^{\mathrm{g}}\,\hat{\mathbf{U}}_J^{\mathrm{g}}. \tag{26}$$

From (26) it is evident that all the natural BCs are satisfied in the strong sense, no numerical integration is used in the procedure. Therein, the matrices $\mathbf{B}$, $\mathbf{H}$ and $\mathbf{G}$ are compatibility matrices consisting of first-order derivatives of shape functions. Since the IMLS approximation is used the essential BCs are satisfied by a standard procedure as in FEM.

4 NUMERICAL EXAMPLE

4.1 AXIAL BAR

In order to verify the presented methods a benchmark example of the bar in gradient elasticity subjected to the axial load, displayed in Fig. 2, is considered. The problem of gradient elasticity is governed by the differential equation (1). The bar has the cross-section surface $A=1$ and the length $L=1$. The Young's modulus is taken as $E=1$. The left side of the bar is clamped, while on the right side the force $P_0=1$ is applied, as seen in Fig. 2. For the mixed Meshless Finite Volume Method (mMFVM) the utilized BCs are $u(0)=0$, $R(0)=-l^2Eu''(0)=0$, $u'(L)=\varepsilon_o=0.5$ and $P(L)=Eu'(L)-l^2Eu'''(L)=P_0$. Here, P and R stand for the generalized tractions and double-tractions, respectively.

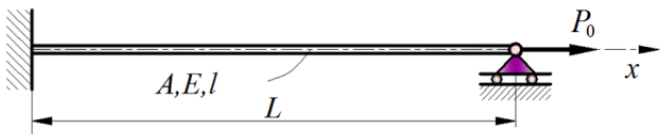

Figure 2: Axial bar in gradient elasticity

In the mMFVOSM and mMCOSM, BCs are modified. Herein, the gradient elasticity problem is governed by second-order differential equations (7) and (8). Therein, the BCs of the classical problem are defined as $u_{\mathrm{c}}(0)=0$ and $t_{\mathrm{c}}(L)=P_0$, while the BCs of the gradient problem are $u_{\mathrm{g}}(0)=0$ and $u_{\mathrm{g}}(L)=u_{\mathrm{g}}^{\mathrm{AN}}$. Herein, the value of the gradient displacement at the right-hand-side of the bar, at $x=L$, is dependent on the parameter l and is calculated from the analytical solution [21]. Numerical calculations using presented mixed meshless procedures have been done. For the approximation of the unknown variables only the first-order basis in the IMLS functions is used. For computing purposes, discretizations using uniformly distributed nodes are applied. The influence of the parameter l on the deformation responses of the bar has been investigated and the obtained distributions for the displacement and strain are compared with the analytical solutions [21] as portrayed in Fig. 3 and Fig. 4.

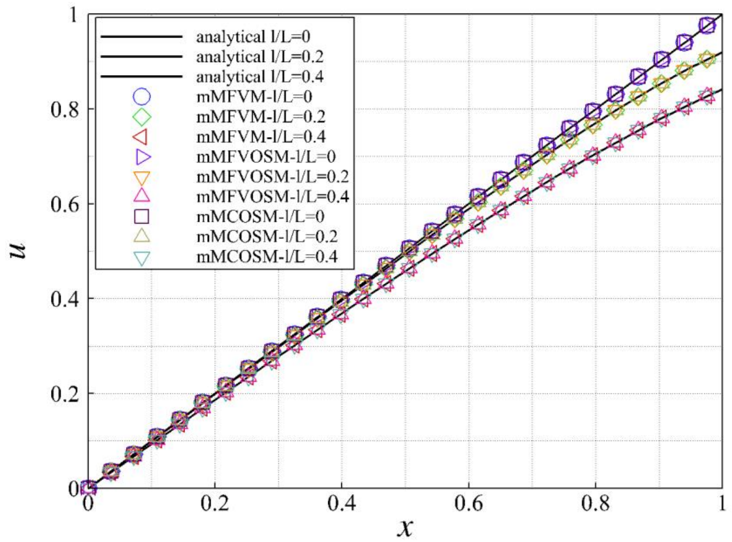

Figure 3: Axial bar - distribution of displacement

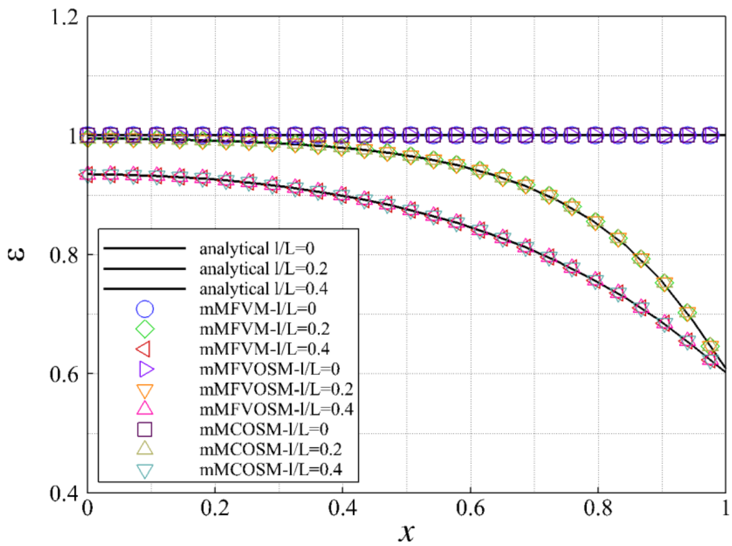

Figure 4: Axial bar - distribution of strain

As evident, the obtained results are accurate and analytical distributions are captured correctly using all the presented mixed meshless procedures. Thus, these methods show considerable potential for applications in high dimensional structures, where gradient elasticity is a necessity. Some of these phaenomena include the modeling of size effects in structures and capturing accurate stress distributions near the crack tip in fracture problems.

5 CONCLUSION

Three different meshless methods based on the mixed MLPG stratagem for solving gradient elasticity have been proposed and applied for solving simple problems in 1D gradient elasticity. In first two mixed meshless methods, the Heaviside function is chosen as the test function leading to the forms of the mixed Meshless Finite Volume Method (mMFVM). In the third method the Dirac delta function is utilized as the test function leading to a mixed meshless collocation method. The first method (mMFVM) is based on the modification of the original fourth-order governing equation of the gradient elastic bar by employing a mixed approach, where displacements and the higher-order gradients are approximated separately, while the second (mMFVOSM) and third (mMCOSM) method are based on the application of the operator split procedure and a staggered solution of the original problem. For the approximation of all unknown field variables IMLS is utilized. In mMFVM, all BCs are satisfied in the weak sense, while in mMFVOSM a reduction of the equation system is performed, and the essential BCs are imposed directly, as in FEM. In the mMCOSM all the BCs are enforced in the strong form at the collocation nodes. The presented mixed meshless methods have been tested on one benchmark example dealing with the axially loaded bar with gradient elasticity and it has been shown that all methods yield very accurate responses even for the first-order meshless approximation functions. The obtained results imply that the proposed mixed MLPG strategies have considerable potential for solving engineering problems governed by high-order differential equations. It is to note that the application of the mixed MLPG strategy lowers the continuity requirements on the trial functions, which in general reduces the computational time and increases numerical robustness. Thus, in future research the presented methods will be extended and utilized for solving gradient elasticity problems in higher-dimensions.

ACKNOWLEDGEMENTS

The second author would like to acknowledge the Fulbright Scholarship that allowed him to stay at UCI during his research. This work has also been partly supported by Croatian Science Foundation under the project Multiscale Numerical Modeling of Material Deformation Responses from Macro- to Nanolevel (2516).

REFERENCES

[1] G. Engel, K. Garikipati, T.J.R. Hughes, M.G. Larson, L. Mazzei, R.L. Taylor, Continuous/discontinuous finite element approximations of fourth-order elliptic problems in structural and continuum mechanics with applications to thin beams and plates, and strain gradient elasticity, Computer Methods in Applied Mechanics and Engineering, 191 (2002) 3669-3750.

[2] P. Fischer, J. Mergheim, P. Steinmann, On the C1 continuous discretization of non-linear gradient elasticity: A comparison of NEM and FEM based on Bernstein–Bézier patches, International Journal for Numerical Methods in Engineering, 82 (2010) 1282-1307.

[3] E. Amanatidou, N. Aravas, Mixed finite element formulations of strain-gradient elasticity problems, Computer Methods in Applied Mechanics and Engineering, 191 (2002) 1723-1751.

[4] A. J. Salgado, J. Guzmán, F.-J. Sayas, A Note on the Ladyzenskaja-Babuska-Brezzi Condition, Journal of Scientific Computing, 56 (2012) 219-229.

[5] G.R. Liu, Y.T. Gu, An Introduction to Meshfree Methods and Their Programming, Springer, Dordrecht, The Netherlands, 2005.
[6] P. Krysl, T. Belytschko, Analysis of thin plates by the element-free Galerkin method, Computational Mechanics, 17 (1995) 26-35.
[7] S.N. Atluri, J.Y. Cho, H.-G. Kim, Analysis of thin beams, using the meshless local Petrov–Galerkin method, with generalized moving least squares interpolations, Computational Mechanics, 24 (1999) 334-347.
[8] T. Jarak, J. Soric, Analysis of rectangular square plates by the mixed Meshless Local Petrov-Galerkin (MLPG) approach, CMES: Computer Modeling in Engineering & Sciences, 38 (2008) 231-261.
[9] S.N. Atluri, Z.D. Han, A.M. Rajendran, A New Implementation of the Meshless Finite Volume Method, Through the MLPG "Mixed" Approach, CMES: Computer Modeling in Engineering & Sciences, 6 (2004) 491-514.
[10] M.R. Moosavi, F. Delfanian, A. Khelil, The orthogonal meshless finite volume method for solving Euler–Bernoulli beam and thin plate problems, Thin-Walled Structures, 49 (2011) 923-932.
[11] H. Askes, I. Morata, E.C. Aifantis, Finite element analysis with staggered gradient elasticity, Computers & Structures, 86 (2008) 1266-1279.
[12] C.Q. Ru, E.C. Aifantis, A simple approach to solve boundary-value problems in gradient elasticity, Acta Mechanica, 101 (1993) 59-68.
[13] T. Most, C. Bucher, A Moving Least Squares weighting function for the Element-free Galerkin Method which almost fulfills essential boundary conditions, Structural Engineering and Mechanics, 21 (2005) 315-332.
[14] H.-Y. Hu, A.H.-D. Cheng, Radial basis collocation methods for elliptic boundary value problems, Computers & Mathematics with Applications, 50 (2005) 289–320.
[15] S.N. Atluri, H.T. Liu, Z.D. Han, Meshless local Petrov-Galerkin (MLPG) mixed collocation method for elasticity problems, CMES: Computer Modeling in Engineering & Sciences, 14 (2006) 141-152.
[16] B. Jalušić, Meshless numerical method for modeling of heterogeneous structures, Faculty of Mechanical Engineering and Naval Architecture, Zagreb, 2016.
[17] G.R. Liu, Mesh Free Methods: Moving beyond the Finite Element Method, CRC Press, Boca Raton,USA., 2003.
[18] S.N. Atluri, The Meshless Method (MLPG) for Domain & BIE Discretization, Tech Science Press, Forsyth, USA, 2004.
[19] T. Jarak, J. Soric, J. Hoster, Analysis of shell deformation responses by the meshless local Petrov-Galerkin (MLPG) approach, CMES: Computer Modeling in Engineering & Sciences, 18 (2007) 235-246.
[20] T. Most, C. Bucher, New concepts for moving least squares: An interpolating non-singular weighting function and weighted nodal least squares, Engineering Analysis with Boundary Elements, 32 (2008) 461-470.
[21] S. Papargyri-Beskou, D. Beskos, Static Analysis of Gradient Elastic Bars, Beams, Plates and Shells, 2010.